

Incommensurate magnetic ordering in $\text{Cu}_2\text{Te}_2\text{O}_5\text{X}_2$ (X=Cl, Br) studied by neutron diffraction

O. Zaharko,^{*} A. Daoud-Aladine, S. Streule, J. Mesot
Laboratory for Neutron Scattering, ETHZ & PSI, CH-5232 Villigen, Switzerland

P.-J. Brown
Institut Laue-Langevin, 156X, 38042 Grenoble Cédex, France

H. Berger
Institut de Physique de la Matière Complexe, EPFL, CH-1015 Lausanne, Switzerland
(Dated: November 26, 2018)

We present the results of the first neutron powder and single crystal diffraction studies of the coupled spin tetrahedra systems $\text{Cu}_2\text{Te}_2\text{O}_5\text{X}_2$ (X=Cl, Br). Incommensurate antiferromagnetic order with the propagation vectors $\mathbf{k}_{\text{Cl}} \approx [0.150, 0.422, \frac{1}{2}]$, $\mathbf{k}_{\text{Br}} \approx [0.158, 0.354, \frac{1}{2}]$ sets in below $T_N=18$ K for X=Cl and 11 K for X=Br. No simple collinear antiferromagnetic or ferromagnetic arrangements of moments within Cu^{2+} tetrahedra fit these observations. Fitting the diffraction data to more complex but physically reasonable models with multiple helices leads to a moment of $0.67(1)\mu_B/\text{Cu}^{2+}$ at 1.5 K for the Cl-compound. The reason for such a complex ground state may be geometrical frustration of the spins due to the intra- and inter-tetrahedral couplings having similar strengths. The magnetic moment in the Br- compound, calculated assuming it has the same magnetic structure as the Cl compound, is only $0.51(5)\mu_B/\text{Cu}^{2+}$ at 1.5 K. In neither compound has any evidence for a structural transition accompanying the magnetic ordering been found.

PACS numbers: 75.10.Jm, 75.30.-m, 61.12.Ld

Recently much experimental and theoretical effort has been invested in trying to understand low-dimensional quantum spin systems.¹ Reduced dimensionality and frustration in such systems lead to interesting new ground states and spin dynamics. It is known, for example, that one-dimensional (1D) dimerized or frustrated spin chains have gapped singlet ground states. In two-dimensional (2D) spin systems, which include the cuprate high-temperature superconductors, strong renormalization of the spin excitations due to quantum fluctuations has been reported.^{2,3}

The copper tellurates $\text{Cu}_2\text{Te}_2\text{O}_5\text{X}_2$ (X=Cl, Br)⁴ belong to a new family of such compounds. They contain tetrahedral clusters of $\text{S}=\frac{1}{2}$ Cu^{2+} spins aligned in tubes along the c direction and separated by lone pair cations in the ab plane. These systems are therefore ideally suited to study the interplay between the built-in frustration within tetrahedra and magnetic coupling between them. Both compounds crystallize in the non-centrosymmetric tetragonal space group $P\bar{4}$. The four Cu^{2+} ions occupy a single set of general equivalent positions 4(h) ($x \approx 0.730$, $y \approx 0.453$, $z \approx 0.158$). The 4 ions clustered round the origin: Cu1 (x, y, z), Cu2 ($1-x, 1-y, z$), Cu3 ($y, 1-x, -z$) and Cu4 ($1-y, x, -z$) form an irregular tetrahedron with two longer (Cu1-Cu2, Cu3-Cu4) and four shorter edges. The magnetic susceptibility of both compounds shows a broad maximum around 20 K – 30 K and drops rapidly at lower temperatures,⁴ as is typical of spin gapped systems. The strength of the coupling constant obtained by fitting the susceptibility to a model in which the tetrahedra are isolated and all 4 inter-tetrahedral coupling constants have the same strength is 38.5 K and 43 K for

X= Cl and Br, respectively. Further magnetic susceptibility and specific heat measurements⁵ indicate the onset of antiferromagnetic (AF) order in the Cl-compound at $T_N=18.2$ K showing that the inter-tetrahedral coupling is substantial. Interestingly, the magnetic susceptibility is almost isotropic and thermal conductivity studies suggest strong spin-lattice coupling near T_N .⁶ For the Br-compound an unusual phase transition involving low-energy longitudinal magnetic modes around 11.4 K has been inferred from Raman scattering,⁵ which was later attributed to the onset of magnetic order.⁸ Raman light scattering experiments^{7,8} in $\text{Cu}_2\text{Te}_2\text{O}_5\text{X}_2$ compounds have been analyzed using a model in which the ion pairs Cu1-Cu2 and Cu3-Cu4 act as dimers within each tetrahedron. The exchange constants J_1 and J_2 in this model are defined by the spin Hamiltonian

$$H = J_1(\mathbf{S}_1 \cdot \mathbf{S}_3 + \mathbf{S}_1 \cdot \mathbf{S}_4 + \mathbf{S}_2 \cdot \mathbf{S}_3 + \mathbf{S}_2 \cdot \mathbf{S}_4) + J_2(\mathbf{S}_1 \cdot \mathbf{S}_2 + \mathbf{S}_3 \cdot \mathbf{S}_4). \quad (1)$$

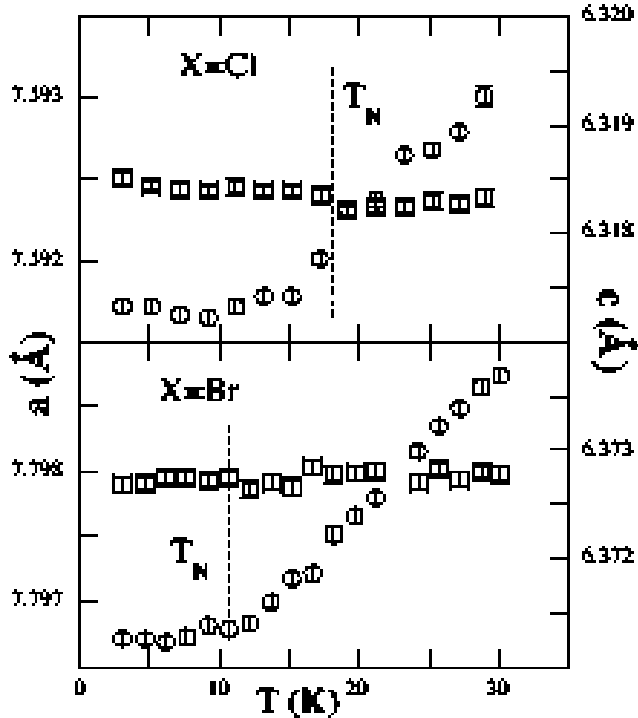
and were determined as: $J_1=47.5$ K and $J_2/J_1=0.7$ for the Br-, and $J_1=40.7$ K and $J_2/J_1=1$ for the Cl-system. Many experimental and theoretical questions about these interesting systems still remain open.^{9–13} Neutron elastic and inelastic scattering may provide answers to some of them by determining the magnetic ground states of the compounds and by probing their spin dynamics. We report here the results of the first neutron diffraction experiments on the compounds. The experiments have been made on powder and single crystal samples of $\text{Cu}_2\text{Te}_2\text{O}_5\text{Cl}_2$ and on powder samples of $\text{Cu}_2\text{Te}_2\text{O}_5\text{Br}_2$. Both systems have been found to exhibit long-range incommensurate magnetic order.

High-purity powders of $\text{Cu}_2\text{Te}_2\text{O}_5\text{X}_2$ and single crystals of $\text{Cu}_2\text{Te}_2\text{O}_5\text{Cl}_2$ were prepared by the halogen vapor transport technique, using TeX_4 and X_2 as transport agents. Neutron powder diffraction (NPD) patterns were collected in the temperature range 1.5 K - 30 K, on the DMC instrument at SINQ, Switzerland, with a neutron wavelength of $\lambda=4.2$ Å (Cl) and $\lambda=2.6$ Å (Br) and on the high-resolution HRPT instrument at SINQ ($\lambda=1.889$ Å). The neutron single crystal diffraction (NSCD) experiments on two crystals of dimensions $2.5 \times 3 \times 15$ mm³ and $2 \times 3.5 \times 6$ mm³ were carried out using the diffractometers TriCS at SINQ ($\lambda=1.18$ Å) and D15 ($\lambda=1.17$ Å) at the high-flux ILL reactor, France.

The evolution of the lattice constants at low temperatures for $\text{Cu}_2\text{Te}_2\text{O}_5\text{X}_2$ X=Cl and Br is presented in Fig. 1. The lattice contraction for both compounds is anisotropic above T_N : the change in the *ab* plane being greater than that along *c*. Below T_N the lattice constants change very little and no splitting or broadening of Bragg peaks, such as would occur in an accompanying structural transition, has been observed.

In $\text{Cu}_2\text{Te}_2\text{O}_5\text{Cl}_2$ below $T_N=18$ K magnetic peaks ap-

FIG. 1: Temperature evolution of the lattice constants from high-resolution HRPT NPD data. Circles denote the *a* and squares the *c* lattice constants.

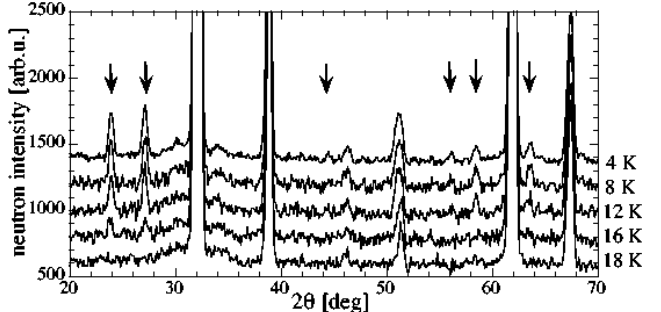


peared (Fig. 2), which cannot be indexed using simple multiples of the crystallographic unit cell, thus implying that the magnetic structure is incommensurate (ICM). The wave vector $\mathbf{k}_{\text{Cl}} \approx [0.150, 0.422, \frac{1}{2}]$ was determined from the single crystal experiment. The magnetic

peaks in the $\text{Cu}_2\text{Te}_2\text{O}_5\text{Br}_2$ NPD patterns appeared below $T_N=11$ K. Their topology is similar to that observed in the Cl-compound and corresponds to the wave vector $\mathbf{k}_{\text{Br}} \approx [0.158, 0.354, \frac{1}{2}]$.

The variation with temperature of the positions and

FIG. 2: DMC neutron powder diffraction patterns of $\text{Cu}_2\text{Te}_2\text{O}_5\text{Cl}_2$. Arrows point to magnetic reflections.



intensities of the lowest angle magnetic peaks of both compounds is shown in Fig. 3. The intensity varies as the square of the $S=\frac{1}{2}$ Brillouin function. The position of the $\text{Cu}_2\text{Te}_2\text{O}_5\text{Br}_2$ peak is almost constant and strictly incommensurate below T_N , whilst that of $\text{Cu}_2\text{Te}_2\text{O}_5\text{Cl}_2$ varies significantly in the vicinity of T_N . The width of the magnetic peaks is resolution-limited, indicating the long-range nature of the magnetic order.

The diffraction experiments on $\text{Cu}_2\text{Te}_2\text{O}_5\text{Cl}_2$ single crystals allowed us to clarify the magnetic symmetry and enumerate the magnetic domains. The star of the wave vector $\mathbf{k}=(\alpha, \beta, \frac{1}{2})$ in the space group $P\bar{4}$ has four arms shown by the black lines in Fig. 4a. Each arm gives rise to a configuration domain; all have the same structure but possibly different populations. In the crystal investigated on the TriCS instrument the only satellites observed were the pairs $H \pm \mathbf{k}$ around each nuclear Bragg reflection H , so the 90 deg rotation domains are not present. In the crystal investigated on D15 not only were all four satellites around each H observed, but in addition, another star of the wave vector $\mathbf{k}' \approx [-0.15, 0.42, \frac{1}{2}]$ was present. The \mathbf{k} and \mathbf{k}' vectors are not related by the symmetry elements of the group $P\bar{4}$, so the magnetic structures associated with these two stars must be different. Pairs of vectors from the two stars may combine to generate a $\mathbf{k} - \mathbf{k}'$ structure. Careful comparison of the integrated intensities in the \mathbf{k} and \mathbf{k}' data sets reveals that the ratio of intensities of satellites based on the same H for \mathbf{k} and \mathbf{k}' is different.

In what follows we describe attempts to develop independent models for the \mathbf{k}' structure from 59 reflections of the ILL data set and for the \mathbf{k} structure based on 18(25) magnetic reflections from the ILL (TriCS) data sets. It is worth noting that simple antiferromagnetic or ferromagnetic arrangements are not compatible with the ICM wave vector. The lack of local symmetry at the 4(h) position and the ICM wave vector implies that the

FIG. 3: Temperature evolution of the lowest angle magnetic peak ($\approx \alpha, \beta, \frac{1}{2}$) of Cl (squares) and Br (circles) compounds from DMC NPD data. Top: peak position in [deg.], bottom: integrated intensities, normalized to the low temperature value. The solid line represents the square of the $S=\frac{1}{2}$ Brillouin function.

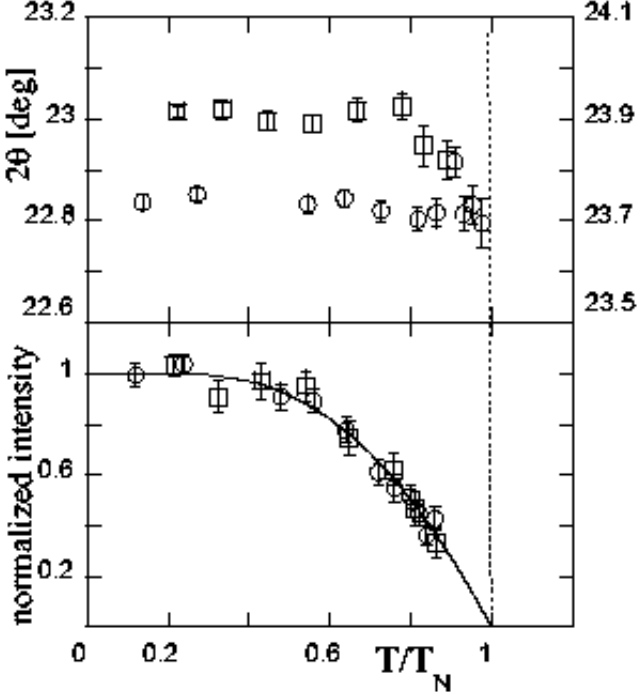
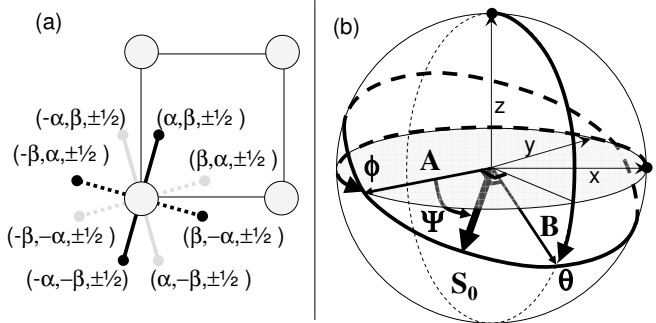


FIG. 4: a) The [001] projection of reciprocal space for the $\text{Cu}_2\text{Te}_2\text{O}_5\text{Cl}_2$ structure. Black points correspond to \mathbf{k} and grey - to \mathbf{k}' magnetic reflections. b) Definition of the angles for the helical spin structure.



magnetic moments of the four Cu^{2+} ions in the cell are independent. The commensurate $k_z = \frac{1}{2}$ means that corresponding spins in successive unit cells along the c -axis are oppositely oriented.

In an ICM structure the moment \mathbf{S}_{jl} of the j th ion in the l th unit cell can be expressed as

$$\mathbf{S}_{jl} = \mathbf{A}_j \cos(\mathbf{k} \cdot \mathbf{r}_l + \psi_j) + \mathbf{B}_j \sin(\mathbf{k} \cdot \mathbf{r}_l + \psi_j) \quad (2)$$

The spin components are modulated by the propagation vector \mathbf{k} . \mathbf{r}_l is the radius vector to the origin of the l th unit cell. \mathbf{A}_j and \mathbf{B}_j are orthogonal vectors which define the magnitude and direction of the axes of the modulation on the j th atom, whilst ψ_j defines its phase. If B (or A)=0, the structure is amplitude modulated: the magnetic moment of each ion has a constant direction and varies sinusoidally from cell to cell. Attempts to fit the data using such models led to unreasonably high moments ($>1 \mu_B/\text{ion}$) at the wave maximum.

All other situations describe more complex magnetic structures in which the spin j rotates from cell to cell in the plane defined by \mathbf{A}_j and \mathbf{B}_j . If $|\mathbf{A}_j| \neq |\mathbf{B}_j|$ the rotating spins j have an elliptical envelope in the $(\mathbf{A}_j, \mathbf{B}_j)$ plane. When all the $(\mathbf{A}_j, \mathbf{B}_j)$ planes are orthogonal or parallel to the propagation vector, the specific structures are usually referred to as helices or cycloids, respectively. If $|\mathbf{A}_j| = |\mathbf{B}_j|$ the envelope becomes circular and the atoms of site j have the same moment in each cell. We refer to this model with constant moments as the generalized helix model.

A generalized helical spin arrangement is fully characterized by defining, for each independent atom, the amplitude $|A| = |B|$, two angles defining the plane in which the spins rotate and the phase of the modulation. The angles chosen are the polar coordinates θ_j, ϕ_j of \mathbf{B}_j and the phase angle ψ_j (see Fig. 4b). The vector \mathbf{A}_j can always be chosen in the ab plane ($\theta_{\mathbf{A}_j}=90^\circ$); orthogonality of \mathbf{A}_j and \mathbf{B}_j is ensured by making $\phi_{\mathbf{A}_j}=\phi_{\mathbf{B}_j} + 90^\circ$. ψ_j is the angle between \mathbf{S}_{j0} and \mathbf{A}_j . This description requires 12 independent parameters within the physically reasonable assumption that all the Cu^{2+} moments are equal. A simulated annealing algorithm which provides a general purpose optimization technique to resolve this kind of large combinatorial problem^{14,15} was used to generate possible models which could subsequently be refined by a least squares procedure.¹⁶

In one class of models, collinear arrangements of the Cu spins within a tetrahedron was imposed. This may result in either a tetramer with $S_{tet}=0$ ($J_1 \gg J_2$) or two dimers with $S_{dim}=0$ ($J_1 \ll J_2$). These models would assume that the dominant coupling is antiferromagnetic. Such AF exchange is poorly justified since: in the first case the J_1 coupling is associated mainly with the Cu-O-Cu path, with an angle Cu-O-Cu approximately 110 deg. In the second case, the path associated with the J_2 coupling is even more complex, possibly involving the halogen orbitals. We therefore also tried collinear arrangements which could arise from FM or partial FM exchange. None of the collinear arrangements give a reasonable fit to the experimental observations and models based on tetramers or dimers can therefore be discarded. Much better fits to the data were obtained for models in which the 4 Cu^{2+} moments in each tetrahedron form two canted pairs: Cu1-Cu2 and Cu3-Cu4. The pairs share a common $(\mathbf{A}_j, \mathbf{B}_j)$ plane but the associated helices have different phases ψ_j (see Table I). The difference between the phases defines the canting angle between spins of the

pair α and this angle is the same for all tetrahedra in the structure. Using this model (Fig. 5) and the propagation vector \mathbf{k}' we obtained $\alpha_{12}=38(6)$ deg, $\alpha_{34}=111(14)$ deg and $m_{12}=1.27(6) \mu_B/\text{pair}$, $m_{34}=0.76(14) \mu_B/\text{pair}$. The refined moment value of the Cu^{2+} ions is $0.67(1) \mu_B/\text{ion}$ and the magnetic reliability factor R_M is 10.7% for this model.

Surprisingly, the above model does not give a good fit to the intensities of reflections indexed with the \mathbf{k} wave vector; the relative arrangement of the pairs in the \mathbf{k} and \mathbf{k}' structures must be different. Unfortunately the \mathbf{k} data sets are too limited to allow a final model for this wave vector to be proposed. But these findings indicate that a number of ground states with equal or close energies might exist.

The complexity of the \mathbf{k}' magnetic structure implies a delicate interplay involving geometrical frustration, between the different couplings within the tetrahedra and the quite significant inter-tetrahedral interaction. These together with the antisymmetric Dzyaloshinskii-Moriya anisotropy interactions define the final spin arrangement. The model can account for the almost isotropic magnetic susceptibility⁶, and gives support to the coexistence of AF and 90-deg couplings, that was first proposed from Raman experiments.⁸ The presence of the ‘canted pair’ motif might suggest that the J_2 interaction prevails in the competition between all the above mentioned interactions. However, this question can be left open for future study.

The spin arrangement in $\text{Cu}_2\text{Te}_2\text{O}_5\text{Br}_2$ cannot be determined from the available NPD data. The magnetic moment derived, assuming the same magnetic structure as for the Cl-compound, is only $0.51(5) \mu_B/\text{Cu}^{2+}$ at 1.5 K, much less than in $\text{Cu}_2\text{Te}_2\text{O}_5\text{Cl}_2$. This low value may indicate that the Br-compound is closer to the quantum critical point than the Cl-analogue.⁵⁻⁷ However, the similarity of the magnetic wave vectors does not guarantee the same magnetic structure for the two systems. Single crystal experiments with a high flux neutron diffractometer are necessary to determine the spin arrangement in the Br-compound.

We conclude that our neutron powder and single crystal diffraction experiments confirm the existence of long-range magnetic ordering in $\text{Cu}_2\text{Te}_2\text{O}_5\text{X}_2$ compounds below T_N . The magnetic order is propagated with the incommensurate wave vectors $\mathbf{k}_{\text{Cl}} \approx [0.150, 0.422, \frac{1}{2}]$ and $\mathbf{k}_{\text{Br}} \approx [0.158, 0.354, \frac{1}{2}]$. The model proposed for the Cl-compound implies a canting of the spins and the presence of two canted pairs within the tetrahedra. New theoreti-

cal studies are needed to quantify the interplay between spin frustration and quantum fluctuations in these systems.

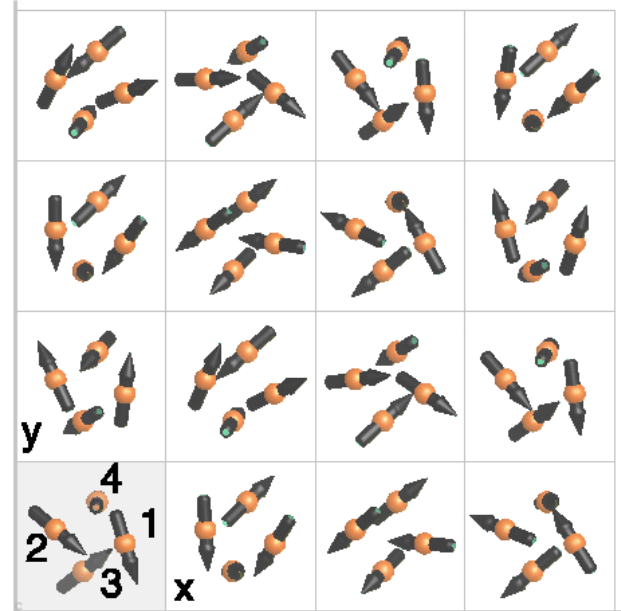
The work was performed at SINQ, Paul Scherrer Institute, Villigen, Switzerland and ILL reactor, Grenoble, France. We thank Drs. M. Prester, H. Ronnow and Profs. A. Furrer, F. Mila for fruitful discussions and Drs. L. Keller, V. Pomjakushin for experimental assistance. The sample preparation was supported by the NCCR re-

TABLE I: The magnetic parameters from neutron diffraction studies of $\text{Cu}_2\text{Te}_2\text{O}_5\text{Cl}_2$.

\mathbf{k}	$0.1505(8), 0.4220(2), \frac{1}{2}$	$0.67(1), \mu_B/\text{Cu}^{2+}$
$\theta_{\mathbf{B}}$	$\phi_{\mathbf{B}}$	ψ, deg
Cu1	57(9)	17(8)
Cu2	57(9)	17(8)
Cu3	139(8)	-49(8)
Cu4	139(8)	-49(8)

search pool MaNEP of the Swiss NSF.

FIG. 5: The xy -projection of the $\text{Cu}_2\text{Te}_2\text{O}_5\text{Cl}_2$ \mathbf{k}' magnetic structure with the spin tetrahedra at $-z$ and z .



* e-mail: Oksana.Zaharko@psi.ch

¹ Magnetic systems with competing interactions, edited by H. T. Diep, World Scientific, Singapore (1994).

² S. M. Hayden *et al.*, Phys. Rev. Lett. **67**, 3622 (1991).

³ H. M. Ronnow *et al.*, Phys. Rev. Lett. **87**, 37202 (2001).

⁴ M. Johnsson *et al.*, Chem. Mater. **12**, 2853 (2000).

⁵ P. Lemmens *et al.*, Phys. Rev. Lett. **87**, 227201 (2001).

⁶ M. Prester, *et al.*, Phys. Rev. B **69**, 180401 (2004).

⁷ C. Gros *et al.*, Phys. Rev. B **67**, 174405 (2003).

⁸ J. Jensen, P. Lemmens, and C. Gros, Europhys. Lett. **64**, 689 (2003).

⁹ W. Brenig, and K. W. Becker, Phys. Rev. B **64**, 214413

(2001).

¹⁰ W. Brenig, Phys. Rev. B **67**, 64402 (2003).

¹¹ R. Valenti *et al.*, Phys. Rev. B **67**, 245110 (2003).

¹² K. Totsuka, and H. - J. Mikeska, Phys. Rev. B **66**, 54435 (2002).

¹³ V. N. Kotov *et al.*, [cond-mat/0404674](https://arxiv.org/abs/cond-mat/0404674) (2004).

¹⁴ J. Rodriguez-Carvajal, Physica B **192**, 55 (1993).

¹⁵ S. Kirkpatrick, C. D. Gelatt, Jr. and M. P. Vecchi, Science **220**, 671 (1983).

¹⁶ P. J. Brown, J. C. Matthewman The Cambridge Crystallography Subroutine Library, 1897.